Journal of Medical Robotics Research, Vol. 3, No. 3 (2018) 1841005 (9 pages)
© World Scientific Publishing Company
DOI: 10.1142/S2424905X18410052

Journal of Medical Robotics Research
http://www.worldscientific.com/worldscinet/jmrr

Journal of Medical Robotics Research

Ontology-Based Surgical Subtask Automation, Automating Blunt Dissection

Dénes Ákos Nagy[*,†,‡], Tamás Dániel Nagy[*], Renáta Elek[*], Imre J. Rudas[*], Tamás Haidegger[*,†]

[*]Antal Bejczy Center for Intelligent Robotics, Óbuda University, Bécsi út 96/B, Budapest 1034, Hungary

[†]Austrian Center for Medical Innovation and Technology (ACMIT), Viktor-Kaplan-Straße 2/1, Building A, Wiener Neustadt 2700, Austria

Automation of surgical processes (SPs) is an utterly complex, yet highly demanded feature by medical experts. Currently, surgical tools with advanced sensory and diagnostic capabilities are only available. A major criticism towards the newly developed instruments that they are not fitting into the existing medical workflow often creating more annoyance than benefit for the surgeon. The first step in achieving streamlined integration of computer technologies is gaining a better understanding of the SP. Surgical ontologies provide a generic platform for describing elements of the surgical procedures. Surgical Process Models (SPMs) built on top of these ontologies have the potential to accurately represent the surgical workflow. SPMs provide the opportunity to use ontological terms as the basis of automation, allowing the developed algorithm to easily integrate into the surgical workflow, and to apply the automated SPMs wherever the linked ontological term appears in the workflow. In this work, as an example to this concept, the subtask level ontological term "blunt dissection" was targeted for automation. We implemented a computer vision-driven approach to demonstrate that automation on this task level is feasible. The algorithm was tested on an experimental silicone phantom as well as in several *ex vivo* environments. The implementation used the da Vinci surgical robot, controlled via the Da Vinci Research Kit (DVRK), relying on a shared code-base among the DVRK institutions. It is believed that developing and linking further building blocks of lower level surgical subtasks could lead to the introduction of automated soft tissue surgery. In the future, the building blocks could be individually unit tested, leading to incremental automation of the domain. This framework could potentially standardize surgical performance, eventually improving patient outcomes.

Keywords: Blunt dissection; Da Vinci Research Kit (DVRK); subtask automation; 3D surgical field reconstruction.

JMRR

1. Introduction

Automation in the field of medicine is already present in many forms, such as programmable insulin pumps, respirators and chest compression devices [1–3]. Most medical domains also apply specific guidelines, such as diagnostic and treatment plans, making medical diagnostics and practice (where these guidelines exist) a standardized process [4]. Particularly in the surgical domain, the emergence of robots allows for new functionalities to be implemented [5]. With predefined treatment plans for common diseases, then with tools for execution, automation could become part of the surgical field as well. Computer-Assisted Surgery is penetrating into the fundamental layers of surgical practice, in the case of some research applications, even replacing the surgeon's hand [6–11]. Moreover, commercial robot systems, such as the MAKO (Stryker Inc., Kalamazoo, MI)

Received 30 September 2017; Revised 9 January 2018; Accepted 26 January 2018; Published xx xx xx. This paper was recommended for publication in JMRR Special Issue on Continuum, Compliant, Cognitive, and Collaborative Surgical Robots by Guest Editors: Elena De Momi, Ren Hongliang and Chao Liu.
Email Address: ‡*denes.nagy@irob.uni-obuda.hu*

and CyberKnife (Accuray Inc., Sunnyvale, CA) already offer autonomous treatment delivery and safety functions [12]. The systematic assessment of autonomous capabilities of surgical robots was proposed recently [13].

Novel research is hindered by the fact that the complexity of surgical procedures requires a high level understanding of the surgical process (SP). Standards and generic plans are only valid until the actual soft-tissue surgery begins: while the surgeon has one initial plan, they later modify that on-the-fly to suit the patient's individual characteristics. Based on this, the first proposals to describe surgical operations as a sequence of tasks were published in 2001 [14]. The term SP has been defined as "a set of one or more linked procedures or activities that collectively realize a surgical objective within the context of an organizational structure", along with the term Surgical Process Model (SPM), "a simplified pattern of an SP that reflects a predefined subset of interest of the SP in a formal or semi-formal representation" [15]. The development of SPMs requires the accurate description of agents in surgery, and therefore results in the creation of complex data/knowledge representation systems. These were named ontologies, and have the potential to accurately represent SPs in a way that they can be analyzed in an automated manner. With the surgical ontologies, some functions of surgery (previously known to be very subjective, such as skill assessment) can be objectively measured [14]. Besides skill assessment, ontologies have a good use in a wide spectrum, including [16]

- evaluation of surgical approaches,
- surgical education and assessment,
- optimization of OR management,
- context-aware systems and
- robotic assistance.

SPMs are able to describe surgery on several granularity levels, starting from task level (at high) to the finest levels (e.g. recording the surgeon's motion primitives) [17]. On the higher abstraction levels, critical and time consuming steps can be identified, then lower level analysis can evaluate the surgeons' economy of movement, providing information on the surgeons' manual skills [18, 19].

Within the work presented here, ontologies have been used to break down surgical procedures into the subtask granularity level. This was chosen because it mostly uses nonprocedure-specific surgical actions (such as "ligating", "clipping", "dissecting", etc.). If such terms can be successfully automated, then they can later serve as building blocks for a multitude of surgical procedures. Fine granularity levels (surgical motion primitives) were also considered as possible building blocks, yet they did not prove to be the ideal soution for numerous reasons. While previous works have demonstrated that automation is possible on these levels, where surgical robots perform reaching, pulling, cutting and other primitive motions to achieve a well-defined goal [7], we found that these fine granularity level applications are hard to be used as surgical building blocks, mainly because inter-patient variability makes their target goals — in real world scenarios — difficult to exactly define. Furthermore, as Reiley [18] showed, expert surgeons use fewer movements compared to novices and residents, therefore, instead of focusing on the reproduction of surgical motions, subtask automation should also aim for minimizing tool motion. Finally, working with motion primitives would require a more technical understanding from the surgeon's side, while subtask level terms are abstract enough for surgeons to build up complex procedures. Automating subtask level building blocks enables unit testing of the elements, which would enable the development of safety standards for these procedures, eventually standardizing surgical performance [20].

This paper presents the automated execution of the "blunt dissection" ontological term, as a demonstration that subtask level automation is feasible in surgery. The structure of the paper is as follows: in Sec. 2, a short description of the blunt dissection procedure is given. After presenting the medical background, the computer vision approach is introduced. Next, the surgical robot's control structure is discussed. Section 3 discusses the accuracy of the automation during various scenarios, followed by the conclusion.

2. Materials and Methods

For this work, we choose Laparoscopic Cholecystectomy (LC) as the targeted procedure. Our choice was based on the fact that this procedure is an often studied and well-understood intervention [21]. Based on the surgical literature [22] and video recordings of the procedure, we built a subtask level SPM, and from this description, we selected the "blunt dissection" ontological term for further examination. In our application, this term is handled as an atomic executable task, where the algorithm filling this block defines the set of required sensory inputs to successfully control and monitor the execution of the process. Our process execution consists of requesting a start and an end point from the surgeon (selected on the endoscopic image). After these boundary parameters are set, the program's computer vision element reconstructs the three-dimensional (3D) field and identifies the dissection line between the boundary points. From this line, the computer vision algorithm selects one point with the least depth, on which the robot control executes blunt dissection. After the dissection is complete, the program checks if the target anatomy is exposed. If further dissection is needed, the algorithm reinitiates the dissection line and starts the process again.

2.1. *Blunt dissection*

Blunt dissection is defined as an SP, where the surgeon intends to separate two layers of loosely connected tissue without damaging either. A dissector is gently inserted between the two layers, then the opening of the dissector forces the two layers apart, while braking only the more fragile connective tissue between the layers. It should be noted that surgeons use the name "blunt dissection" for other maneuvers as well, such as peeling a thin layer of connective tissue bluntly. While these also resemble the SP described above, we do not intend to cover all of these cases in our application.

During LC, one prominent use of blunt dissection is for opening up Calot's triangle. This step is one of the key moments, as the Calot's triangle incorporates several vessels and bile ducts, and damaging these structures may lead to serious complications. Besides LC, several other procedures employ blunt dissection as well. Tumor removals (e.g. of thyroid cancer) use blunt dissection to peel away the tumor tissue from the healthy structures.

To test our automated blunt dissection algorithms, a special phantom was created. It consists of two outer layers of hard silicone, and between them a layer of softer, foamy, dissectible layer of silicone. This internal layer can be penetrated easily with the laparoscopic tool and dissection can be carried out. Our experimental setup is shown in Fig. 1.

2.2. *Computer vision*

During robotic minimally invasive (da Vinci-type) laparoscopic surgery, the most common — in some cases the only — sensory input is the stereo endoscopic camera image feed. Due to this fact, we decided to base our algorithm only on the video feed, and not to rely on any additional sensors. In the future, this makes the platform easily integratable into the surgical workflow.

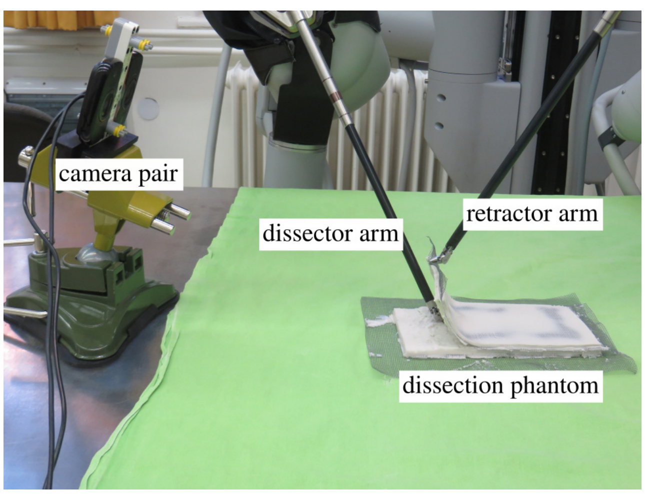

Fig. 1. Automatized blunt dissection test setup, consisting of the da Vinci Surgical System with the DVRK, a dissection phantom and a stereo camera.

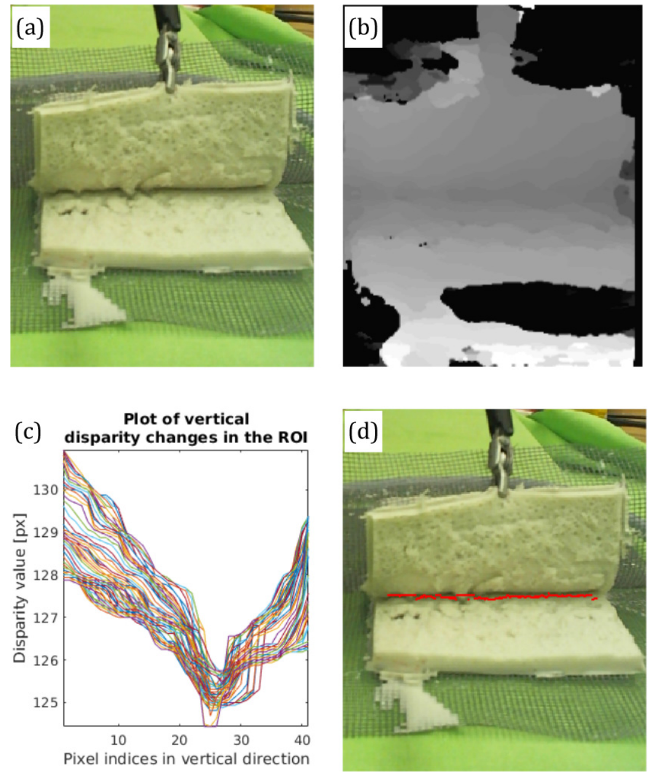

Fig. 2. Computer vision-based automated blunt dissection: (a) stereo camera image of the blunt dissection phantom; (b) disparity map of the surgical field; (c) plot of disparity changes in the vertical direction and (d) blunt dissection profile from the local minimas of the disparity.

During the experiments, we obtained the stereo camera feed using two low-cost web cameras (*Logitech C525 — Logitech*, *Romanel-sur-Morges*, *Switzerland*). The cameras were placed in a stable frame with 50 mm base distance from each other. The blunt dissection phantom was fixed on a stiff surface, approximately 350 mm from the stereo camera. While the distance between an endoscope's two channels is significantly smaller than the one we used in this setup, we compensate for this deviation by placing the camera farther away from the target than it is usual for endoscopes.

The web cameras each provided a 640×480 pixel resolution video feed with fixed focal length. This video stream was then sent to a nearby PC where the computer vision method was implemented in MATLAB 2016b.

Prior to executing the blunt dissection, to achieve accurate 3D representation of the dissection profile, we performed the stereo camera calibration and stereo image rectification. This calibration process was carried out with 19 pairs of images of a checkerboard pattern (grid size: 25×25 mm) fixed on a flat surface. After the capturing of each stereo image, the checkerboard was moved to a new position (and orientation) within the expected target area. The camera calibration and the calculation of the reprojection errors were performed using the MATLAB Stereo Camera Calibrator App. The app projects the checkerboard grid points from the world coordinate system back onto the image coordinates, then compares the resulted point to the original, and accepts it if the error is within one pixel [23].

We validated the camera calibration with the mean pixel error from 10 calibrations. Each calibration used 19 image pairs of whom averagely 2.2 pairs were rejected because of outlier or checkerboard detection errors. During the calibration tests, an average of 0.104 mean pixel error from the 10 cases was achieved, with a standard deviation of 0.0165.

The 3D field reconstruction algorithm was tested on a planar white and a checkerboard pattern placed at different distances (Fig. 3). The mean error was 4.1 mm with 0.7 mm standard deviation. The accuracy of the robot was also tested on 10 cases, where we reached 2.2 mm accuracy with 0.5 mm standard deviation when moving on the image plane and 1 mm accuracy with standard deviation of 0.6 mm on the depth axis.

Following this initialization, the dissection algorithm starts with the user initializing the start and stop points of the blunt dissection line on the initial (two-dimensional (2D)) view. This step serves to define the region of interest (ROI) for the program because the observed surgical field (most of the times) contains more than one candidates where the dissection could be carried out.

From the stereo rectified grayscale images, the program calculates the disparity map, where each disparity value represents the distance between the corresponding pixels on the stereo images. The disparity map is generated using the Semi-Global Block Matching (SGBM) algorithm. SGBM is a highly robust pixelwise matching algorithm based on mutual information and the approximation of a global smoothness constraint [10].

Between the initialized start and stop points, the program defines the precise dissection target points.

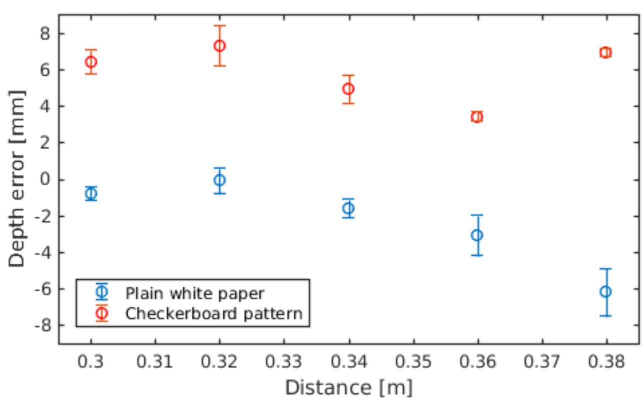

Fig. 3. Depth error of the checkerboard pattern and plain white paper from different distances.

These target points are identified by searching for the local minima on the disparity map (the surface is smoothed using a moving average filter) around the line connecting the initialized boundary points. If the method failed to find peaks, or the disparity values were invalid, the algorithm uses the initial start point and the nearest valid disparity value. After the detection of the dissection line, the program's preciseness is further enhanced by removing the outliers using a Hampel filter. Finally, on the final dissection line, the algorithm chooses the smallest depth point as the next target, resulting in an evenly deepening dissection line.

Besides selecting the 3D points of the intended dissection line, the algorithm also determines the required entry orientation of the dissector tool, by calculating the local direction of the dissection profile (e.g. the orientation points in the direction of the avg. depth gradient).

One of the most challenging issues during the dissection process is the constantly changing environmental factors such as changing external and internal lighting, noise, etc. The laparoscopic environment fortunately reduces these external light sources and the laparoscope's light stays relatively stable. To reduce errors from small shifts in the target's position, we developed a segmentation method which is responsible to accurately define the ROI. This method uses the depth parameters of the dissection line's start and end points.

2.3. *Robot control*

In this work, we used the da Vinci surgical system alongside with the da Vinci Research Kit (DVRK), which provides an open source ROS interface to the robot [24–26]. We choose the da Vinci surgical system because it is widely used in the everyday clinical practice worldwide, with yearly more than 500,000 procedures performed only in the US.

To achieve accurate tool movements based only on the visual information, first, the transformation between the coordinate system of the robot and the camera is determined. For this goal, we use a checkerboard method, where a small, easily detectable checkerboard pattern is attached to the tooltip [27]. Images were captured by both cameras simultaneously in different tool positions, and tool coordinates were calculated from the detected checkerboard positions on the stereo images. Simultaneously, the Cartesian positions were also logged from the DVRK in the robot's coordinate system, after which the transformation between the two coordinate frames is calculated by rigid frame registration.

To separate the tissue layers, the top layer is placed under a constant retraction force. We consider retraction to be a separate subtask from blunt dissection, therefore during the initial tests, it has been executed manually (this is a realistic assumption since retraction is often

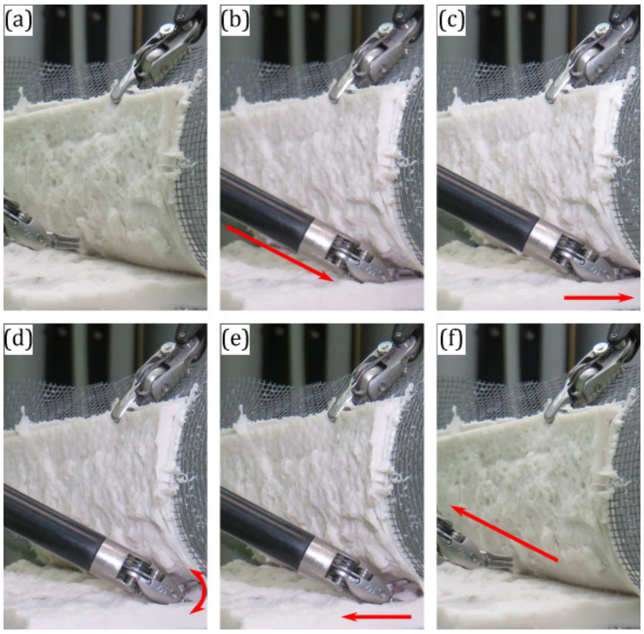

Fig. 4. Robot movements of the surgical subtask automation: (a) the field of view is unobstructed; (b) the surgical instrument moving to the dissection target; (c) penetrating the phantom with the instrument; (d) open the tool; (e) pull out the instrument and (f) move to the next target.

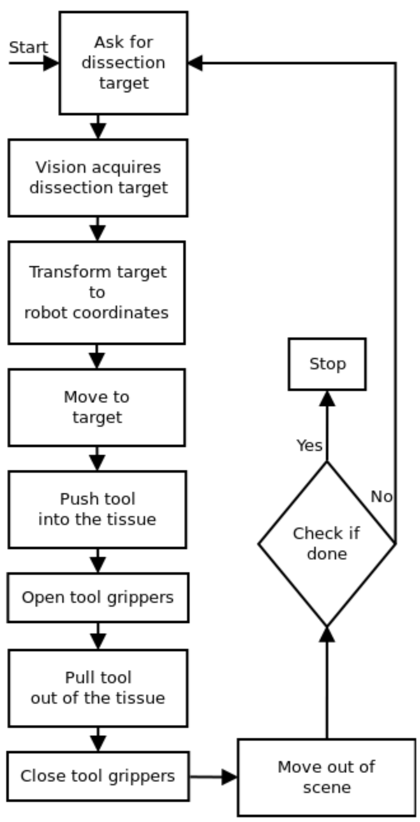

Fig. 5. Flow diagram of the blunt dissection automation method. The image-based input defines the targets of the blunt dissection; based on this information, the robot can perform the blunt dissection surgical subtask.

assigned to the assistant). The workflow of the automatic blunt dissection starts by the computer vision algorithm finding the target on the phantom. The dissector arm then approaches the target, and the tool is moved into the penetrable tissue between the two hard silicone layers. When the tool finishes the penetration of the dissectible tissue, the grippers are opened and the tool is pulled out (remaining open until it left the phantom). The process separates the two tissue layers in the tool's small local region. After this series of movements, the grippers are closed and the tool is moved out of the scene, so it is not obstructing the camera view, and allows a new stereo image to be captured about the surgical field. If the blunt dissection is not finished (e.g. the target anatomical structure is not exposed), a new dissection target is acquired, otherwise, the agent stops. This process is shown in Fig. 5 and the tool movements are shown in Fig. 4.

3. Results

The method was tested on the above-described phantom. The dissection progressed on the intended dissection line in all the test cases. For dissection, an endowrist "large needle driver" instrument was used, and the procedure progressed on a 10 cm dissection line with an average of 0.5 cm/min speed. The tool placement achieved an approximated 1 mm accuracy during these tests. To test accuracy in a predefined environment, an additional test was performed in the following setup: (1) After calibration, the tool was moved in front of the camera and the tool position was recorded on the camera 3D frame and on the robot's coordinate system as well, then (2) the tool was moved away, and (3) the robot was asked to reach the point on the 3D image record. (4) When the robot finished the approach the tool position was compared to the initial tool position. During this test scenario, from 10 test cases, an average of 2.2 mm accuracy was achieved with a standard deviation of 0.5 mm on the camera view's plane. On the depth axis, the algorithm achieved 1 mm accuracy with standard deviation of 0.6 mm. It is worth to note however that the tests are highly dependent on the vision system, and these results could be improved by using industry standard cameras instead of the current low-cost web cameras. With these low-cost cameras, accuracy problems were often attributed to the focusing system and to low resolutions.

3.1. *3D field reconstruction and sensitivity to texture*

We tested our dissection line detection method's sensitiveness to texture. We used four types of paper (plain white, checkerboard pattern, rough surfaced, kraft paper) and the dissection phantom. We kept the phantom and the papers in the opened state to simulate

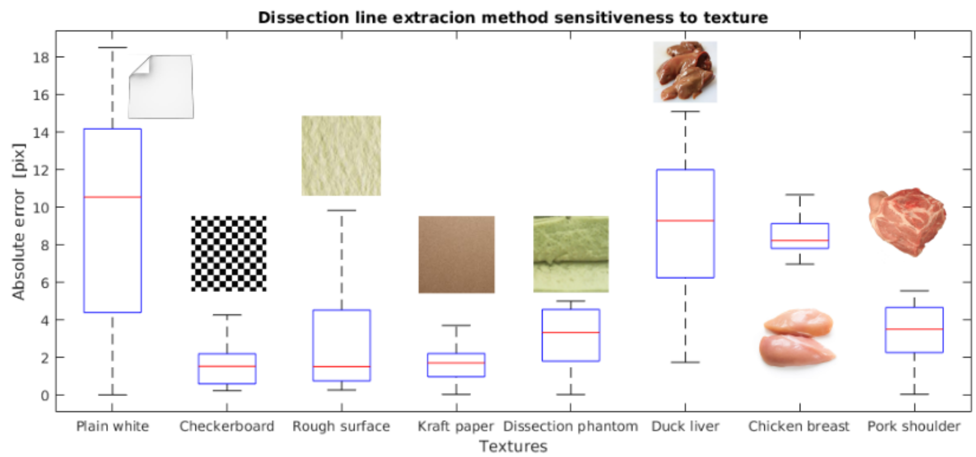

Fig. 6. Dissection line detection sensitiveness to texture.

retraction. In these cases, the algorithm was expected to find a linear dissection profile. We choose the start and end points on the objects with 10 cm distance from each other; these points were the ground truth of the dissection line points. The objects were placed at an approximate 50 cm distance from the stereo system. We found that our method is highly sensitive to the texture and the pattern of the objects. The method worked well on feature rich objects (with the checkerboard pattern, kraft paper and the dissection phantom), but it failed on feature poor objects (plain white paper and rough surface paper). These results are shown in Fig. 6.

We tested the dissection line detection method's sensitiveness to rotation as well. For this, we used the blunt dissection phantom. The phantom was rotated between 0° and 60° with 10° jumps relative to the camera. We found that the method is not significantly sensitive to rotation and performed sufficiently in every case, as it is shown in Fig. 7.

Ex vivo test was conducted on chicken breast, pork shoulder and duck liver in an effort to test the accuracy in a realistic environment. Sensitivity test on the *ex vivo* objects consisted of selecting six points to compare the ground truth with the detected locations. In this experiment, we found that the method is sensitive to the texture of the object and the lighting is crucial. The method worked well on the pork shoulder, and it worked acceptable on the chicken breast and the duck liver. The reason for the pork shoulder's good performance lies in its feature-richness, while the liver and the chicken breast are feature-poor, and glaring for these materials is significant as well, therefore, they provide inferior results (Fig. 8).

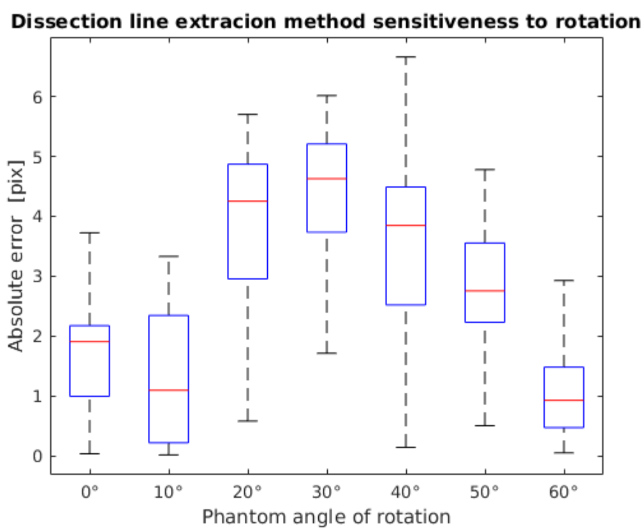

Fig. 7. Absolute error of the dissection line detection while rotating the phantom between 0° and 60° with 10° steps.

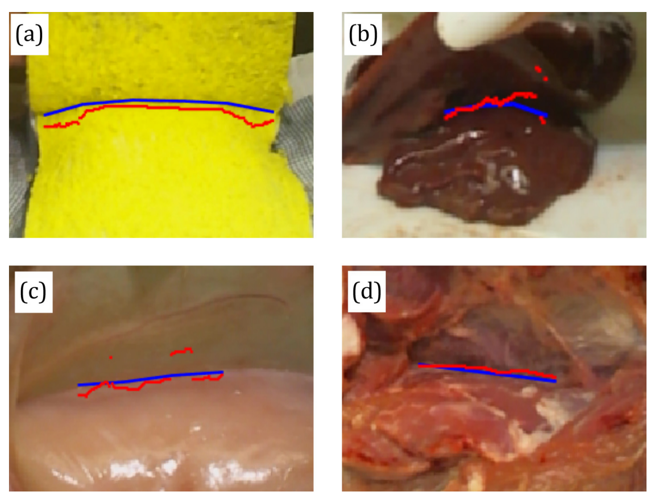

Fig. 8. *Ex vivo* tests of the dissection line detection: (a) blunt dissection silicone sandwich phantom; (b) duck liver; (c) chicken breast and (d) pork shoulder. The method is sensitive to glaring (e.g. liver), and to feature-poor surfaces (e.g. chicken breast).

Finally, the blunt dissection was tested on our silicone sandwich phantom. We requested single dissections at 25 locations along the dissection line. From these 25 test cases, 21 succeeded, and in the remaining 4 cases, the tool missed the exact dissection point by not more than 3 mm.

4. Discussion

The presented method utilizes the readily available stereo camera image feed for the execution of blunt dissection. This makes the algorithm easily integrable into current surgical applications. During initial tests, an average of 1 mm accuracy was achieved, which could further be improved using more reliable stereo cameras. It is worth to note however that in practice, submillimetric accuracy is usually not required for blunt dissection. The presented algorithm does not automate several tasks needed for *ex vivo* and *in vivo* applications. These include the automation of retraction, and the selection of start and stop criteria. In the structure presented above, these are important, but separate subtask level processes, and thus, they should be developed individually. Future objectives include the implementation of "retraction", "suction", "coagulation", etc. ontological terms. In this work, the robot motions were hardcoded into the system, and while they were achieving the intended goal, in future development, we intend to improve the economy of motion by implementing "learning by observation" approaches.

Error monitoring is one of the most important aspects of surgical automation. While other subtask level procedure elements require constant monitoring of the surgical field (for example, the detection of slippage during retraction), such a monitoring is not necessary for blunt dissection. For this application, we expect error monitoring to be an external function which can detect unintended bile leeks or bleeding and interrupts the blunt dissection to start an error handling algorithm.

5. Conclusion

The example of the successfully automated blunt dissection shows that subtask level in SPMs is a low enough granularity level where ontological terms can be defined precisely enough to develop automated algorithms. On the other hand, these terms are widely used in surgical plans, therefore, it can become natural for the surgeons to use these elements to build or assist their surgeries. It was also presented that in case of blunt dissection during LC, the available camera input can provide enough information to execute the automated method solely relying on the visual data. Further trials are necessary to confirm the reliability and robustness of the method under realistic surgical conditions.

Acknowledgments

The authors would like to thank Tivadar Garamvölgyi for providing the phantom used in the experiments. The research was supported by the Hungarian OTKA PD 116121 grant. This work has been supported by ACMIT (Austrian Center for Medical Innovation and Technology), which is funded within the scope of the COMET (Competence Centers for Excellent Technologies) program of the Austrian Government. We acknowledge the financial support of this work by the Hungarian State and the European Union under the EFOP-3.6.1-16-2016-00010 project.

References

1. M. L. Blomquist, Programmable insulin pump, U.S. Patent US6 852 104 B2 (2005).
2. E. A. Hoffman, C. W. H. III and C. F. W. III, Gated programmable ventilator, U.S. Patent US5 183 038 A (1993).
3. U. K. V. Illindala, Chest compression device, U.S. Patent US20 160 310 359 A1 (2016).
4. E. A. Amsterdam, N. K. Wenger, R. G. Brindis, D. E. Casey, T. G. Ganiats, D. R. Holmes, A. S. Jaffe, H. Jneid, R. F. Kelly, M. C. Kontos, G. N. Levine, P. R. Liebson, D. Mukherjee, E. D. Peterson, M. S. Sabatine, R. W. Smalling and S. J. Zieman, 2014 AHA/ACC guideline for the management of patients with non ST-elevation acute coronary syndromes: A report of the American college of cardiology/ American heart association task force on practice guidelines, *Circulation* **130**(25) (2014) e344–e426.
5. M. Hoeckelman, I. Rudas, P. FIorini, F. Kirchner and T. Haidegger, Current capabilities and development potential in surgical robotics, *Int. J. Adv. Robot. Syst.* **12**(61) (2015) 1–39.
6. S. Sen, A. Garg, D. V. Gealy, S. McKinley, Y. Jen and K. Goldberg, Automating multi-throw multilateral surgical suturing with a mechanical needle guide and sequential convex optimization, in *2016 IEEE Int. Conf. Robotics and Automation (ICRA)* (2016), pp. 4178–4185.
7. A. Murali, S. Sen, B. Kehoe, A. Garg, S. McFarland, S. Patil, W. D. Boyd, S. Lim, P. Abbeel and K. Goldberg, Learning by observation for surgical subtasks: Multilateral cutting of 3D viscoelastic and 2D orthotropic tissue phantoms, in *2015 IEEE Int. Conf. Robotics and Automation (ICRA)* (2015), pp. 1202–1209.
8. H. C. Lin, I. Shafran, D. Yuh and G. D. Hager, Towards automatic skill evaluation: Detection and segmentation of robot-assisted surgical motions, *Comput. Aided Surg.* **11**(5) (2006) 220–230.
9. T. Osa, K. Harada, N. Sugita and M. Mitsuishi, Trajectory planning under different initial conditions for surgical task automation by learning from demonstration, in *2014 IEEE Int. Conf. Robotics and Automation (ICRA)* (2014), pp. 6507–6513.
10. H. Hirschmuller, Accurate and efficient stereo processing by semi-global matching and mutual information, in *2005 IEEE Computer Society Conf. Computer Vision and Pattern Recognition (CVPR'05)* (2005), pp. 807–814.
11. Á. Takács, D. Á. Nagy, I. Rudas and T. Haidegger, Origins of surgical robotics: From space to the operating room, *Acta Polytech. Hung.* **13**(1) (2016) 13–30.

12. S. D. Werner, M. Stonestreet and D. J. Jacofsky, Makoplasty and the accuracy and efficacy of robotic-assisted arthroplasty, *Surg. Technol. Int.* **24** (2014) 302–306.
13. T. Haidegger, Scaling the autonomy of surgical robots, in *EEE/RSJ IROS Workshop on Shared Platforms for Medical Robotics Research* (Vancouver, BC, Canada, 2017), pp. 1–3.
14. C. MacKenzie, A. J. Ibbotson, C. G. L. Cao and A. Lomax, Hierarchical decomposition of laparoscopic surgery: A human factors approach to investigating the operating room environment, *Minim Invasive Ther. Allied Technol.* **10**(3) (2001) 121–128.
15. T. Neumuth, S. Schumann, G. Strauß and P. Jannin, Visualization options for surgical workflows, *Int. J. Comput. Assist. Radiol. Surg.* (2006) 438–440.
16. F. Lalys and P. Jannin, Surgical process modelling: A review, *Int. J. Comput. Assist. Radiol. Surg.* **9**(3) (2014) 495–511.
17. T. Neumuth, N. Durstewitz, M. Fischer, G. Strauss, A. Dietz, J. Meixensberger, P. Jannin, K. Cleary, H. Lemke and O. Burgert, Structured recording of intraoperative surgical workflows, in *31st SPIE — The Int. Society for Optical Engineering*, eds. S. C. Horii, O. M. Ratib (SPIE, Bellingham, 2006).
18. C. E. Reiley and G. D. Hager, Task versus subtask surgical skill evaluation of robotic minimally invasive surgery, in *LNCS 5761* (Springer-Verlag, Berlin, Heidelberg, 2009), pp. 435–442.
19. V. Pandey, J. H. N. Wolfe, K. Moorthy, Y. Munz, M. J. Jackson and A. W. Darzi, Technical skills continue to improve beyond surgical training, *J. Vasc. Surg.* **43**(3) (2006) 539–545.
20. T. Haidegger and I. J. Rudas, New medical robotics standards — aiming for autonomous systems, in *IEEE/RSJ Int. Conf. Intelligent Robots and Systems (IROS)* (Vancouver, BC, Canada, 2017), p. WePmPo.14.
21. W. Reynolds, The First laparoscopic cholecystectomy, *J. Soc. Laparoendosc. Surg.* **5**(1) (2001) 89–94.
22. Ö. P. Horváth and J. Kiss, *Littmann Sebészeti Műtéttan* (Medicina, Budapest, 2014).
23. Stereo Calibration App — MATLAB & Simulink, https://www.mathworks.com/help/vision/ug/stereo-camera-calibrator-app.html.
24. G. S. Guthart and J. K. J. Salisbury, The intuitivetm telesurgery system: Overview and application, in *2000 IEEE Int. Conf. Robotics and Automation* (San Francisco, CA, 2000), pp. 618–621.
25. P. Kazanzides, Z. Chen, A. Deguet, G. S. Fischer, R. H. Taylor and S. P. DiMaio, An open-source research kit for the da Vinci® surgical system, in *2014 IEEE Int. Conf. Robotics and Automation (ICRA)* (Institute of Electrical and Electronics Engineers Inc., Hong Kong, China, 2014), pp. 6434–6439.
26. Á. Takács, I. Rudas and T. Haidegger, Open-source research platforms and system integration in modern surgical robotics, *Acta Univ. Sapientiae, Electr. Mech. Eng.* **14**(6) (2015) 20–34.
27. J. B. A. Maintz and M. A. Viergever, A survey of medical image registration, *Med. Image Anal.* **2**(1) (1998) 1–36.

Dënes Ákos Nagy first received his computer engineering degree (BSc) from Pámány Péter Catholic University in 2012. Parallel to his computer engineering studies, he also started his medical degree, and graduated as a Medical Doctor in 2015. After finishing his computer engineering degree, he worked for one year on two photon microscope control softwares. After finishing his MD, he focused on surgal robotics, and started his current PhD at the Antal Bejczy Center for Intelligent Robotics (IRob).

Tamás Dániel Nagy earned his BSc in Molecular Bionics in 2014, and master's degree in Computer Science Engineering in 2016 at the University of Szeged. During his university studies, he joined the Noise Research Group, where he worked on physiological measurements, signal processing and those applications in telemedicine. Since September 2016, he is a PhD student of the Doctoral School of Applied Informatics and Applied Mathematics at Obuda University. He is currently working on the analysis and low level automation of movement patterns in robot surgery interventions.

Renáta Elek received her BSc degree in molecular bionics engineering from the University of Szeged Faculty of Science and Informatics in 2015. During her BSc studies, she worked in the Biological Research Center, where she developed a microfluidic device. She started her MSc studies in 2015 in info-bionics engineering, on the bio-nano instruments and imagers specialization. At the start of her MSc studies, she get acquainted with surgical robotics. She joined the Antal Bejczy Center for Intelligent Robotics surgical robotics group, where she is currently a PhD student working on image-based camera control methods.

Imre J. Rudas is a Doctor of Science of the Hungarian Academy of Sciences, former President of Óbuda University. He is an IEEE Fellow and a Distinguished Lecturer, holder of the Order of Merit of the Hungarian Republic and numerous international and national awards. He is the board member of several international scientific societies, member of editorial boards of international scientific journals, leader of R&D projects and author of more than 750 publications. He is the organizer of a vast number of technical conferences worldwide in the field of robotics, fuzzy logic and system modeling.

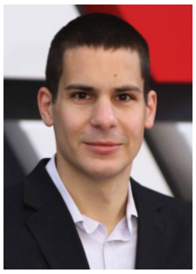

Tamás Haidegger received his MSc degrees from the Budapest University of Technology and Economics (BME) in Electrical Engineering and Biomedical Engineering in 2006 and 2008, respectively. His PhD thesis (2011) was based on a neurosurgical robot he helped in developing when he was a visiting scholar at the Johns Hopkins University. His main fields of research are control/teleoperation of surgical robots, image-guided therapy and supportive medical technologies. Currently, he is an Associate Professor at the Óbuda University, serving as the Deputy Director of the Antal Bejczy Center for Intelligent Robotic. Besides, he is a Research Area Manager at the Austrian Center of Medical Innovation and Technology (ACMIT), working on minimally invasive surgical simulation and training, medical robotics and usability/workflow assessment through ontologies. He is the Co-founder and CEO of a university spin-off — HandInScan — focusing on objective hand hygiene control in the medical environment. They are working together with Semmelweis University, the National University Hospital Singapore and the World Health Organization. Tamás Haidegger is an active member of various other professional organizations, including the IEEE Robotics an Automation Society, IEEE EMBC, euRobotics aisbl and MICCAI. He is a national delegate to an ISO/IEC standardization committee focusing on the safety and performance of medical robots. He has co-authored more than 130 peer reviewed papers published at various scientific meeting and conference proceedings, refereed journals and books in the field of biomedical/control engineering and computer-integrated surgery.